

# Construction of human induced pluripotent stem cell-derived oriented bone matrix microstructure by using *in vitro* engineered anisotropic culture model

Ryosuke Ozasa,<sup>1</sup> Aira Matsugaki,<sup>1</sup> Yoshihiro Isobe,<sup>2</sup> Taro Saku,<sup>2</sup> Hui-Suk Yun,<sup>3</sup> Takayoshi Nakano<sup>1</sup>

<sup>1</sup>Division of Materials and Manufacturing Science, Graduate School of Engineering, Osaka University, 2-1 Yamada-oka, Suita, Osaka 565-0871, Japan

<sup>2</sup>Atree, Inc., 16-12-1 Hiroo, Shibuya-ku, Tokyo 150-0012, Japan

<sup>3</sup>Powder and Ceramics Division, Korea Institute of Materials Science, Changwon, Gyeongnam 642-831, Korea

Received 4 July 2017; revised 1 September 2017; accepted 14 September 2017

Published online 17 October 2017 in Wiley Online Library (wileyonlinelibrary.com). DOI: 10.1002/jbm.a.36238

**Abstract:** Bone tissue has anisotropic microstructure based on collagen/biological apatite orientation, which plays essential roles in the mechanical and biological functions of bone. However, obtaining an appropriate anisotropic microstructure during the bone regeneration process remains a great challenging. A powerful strategy for the control of both differentiation and structural development of newly-formed bone is required in bone tissue engineering, in order to realize functional bone tissue regeneration. In this study, we developed a novel anisotropic culture model by combining human induced pluripotent stem cells (hiPSCs) and artificially-controlled oriented collagen scaffold. The oriented collagen scaffold allowed hiPSCs-derived osteoblast alignment and

further construction of anisotropic bone matrix which mimics the bone tissue microstructure. To the best of our knowledge, this is the first report showing the construction of bone mimetic anisotropic bone matrix microstructure from hiPSCs. Moreover, we demonstrated for the first time that the hiPSCs-derived osteoblasts possess a high level of intact functionality to regulate cell alignment. © 2017 The Authors Journal of Biomedical Materials Research Part A Published by Wiley Periodicals, Inc. J Biomed Mater Res Part A: 106A: 360–369, 2018.

**Key Words:** bone tissue anisotropy, induced pluripotent stem cells, osteoblast arrangement, bone regeneration

**How to cite this article:** Ozasa R, Matsugaki A, Isobe Y, Saku T, Yun H-S, Nakano T. 2018. Construction of human induced pluripotent stem cell-derived oriented bone matrix microstructure by using *in vitro* engineered anisotropic culture model. J Biomed Mater Res Part A 2018;106A:360–369.

## INTRODUCTION

In tissue regeneration, the development of organ-specific architectures is important for the realization of their original functions. Bone tissue has anisotropic-complicated microstructure composed of collagen fibers and biological apatite (BAP), which is an essential contributor to the bone mechanical properties.<sup>1,2</sup> The degree of BAP orientation is well correlated with the Young's modulus of bone tissue.<sup>3</sup> The disruption of bone microstructure often occurs in pathological conditions such as osteoporosis,<sup>4</sup> osteopetrosis,<sup>5</sup> and bone defects,<sup>6</sup> which increases the risk of bone fracture.<sup>7</sup> Bone tissue regeneration requires a rapid recovery of oriented bone matrix architecture, in order to decrease the risk of fractures. However, current treatment approaches to bone regeneration aim at increasing bone mass alone. Reconstructing the bone tissue anisotropy remains a challenge in the field of bone tissue engineering.

Induced pluripotent stem cells (iPSCs), pluripotent cells reprogrammed from somatic cells,<sup>8,9</sup> are a promising source for

the use in tissue engineering and regenerative medicine.<sup>10</sup> iPSCs show pluripotency and self-renewability similar to those of the embryonic stem cells (ESCs) and can differentiate into various types of somatic lineages.<sup>11</sup> iPSCs have overcome some problems associated with the use of ESCs, such as immunogenic rejections and ethical issues. For bone regeneration, a growing number of studies demonstrated that iPSCs can differentiate into osteoblasts both *in vitro*<sup>12</sup> and *in vivo*,<sup>13</sup> suggesting that iPSCs show a potential to advance bone regenerative therapies. Due to the high proliferative capacity of iPSCs, a greater number of cells are available than existing sources of osteoblasts such as mesenchymal stem cells (MSCs)<sup>14</sup> or osteoblasts isolated from patients.<sup>15</sup>

In this study, we developed a novel stem cell culture system by combining human iPSCs (hiPSCs) and anisotropic culture model using oriented collagen substrate (Fig. 1). The strategy of the present culture system is to realize the anisotropic bone tissue which can replace the bone defects, by controlling the cell alignment. Interestingly, we recently

**Conflict of Interest Statement:** The authors have no conflict of interest.

**Correspondence to:** T. Nakano; e-mail: nakano@mat.eng.osaka-u.ac.jp

Contract grant sponsor: Japan Society for the Promotion of Science (JSPS); contract grant number: JP25220912

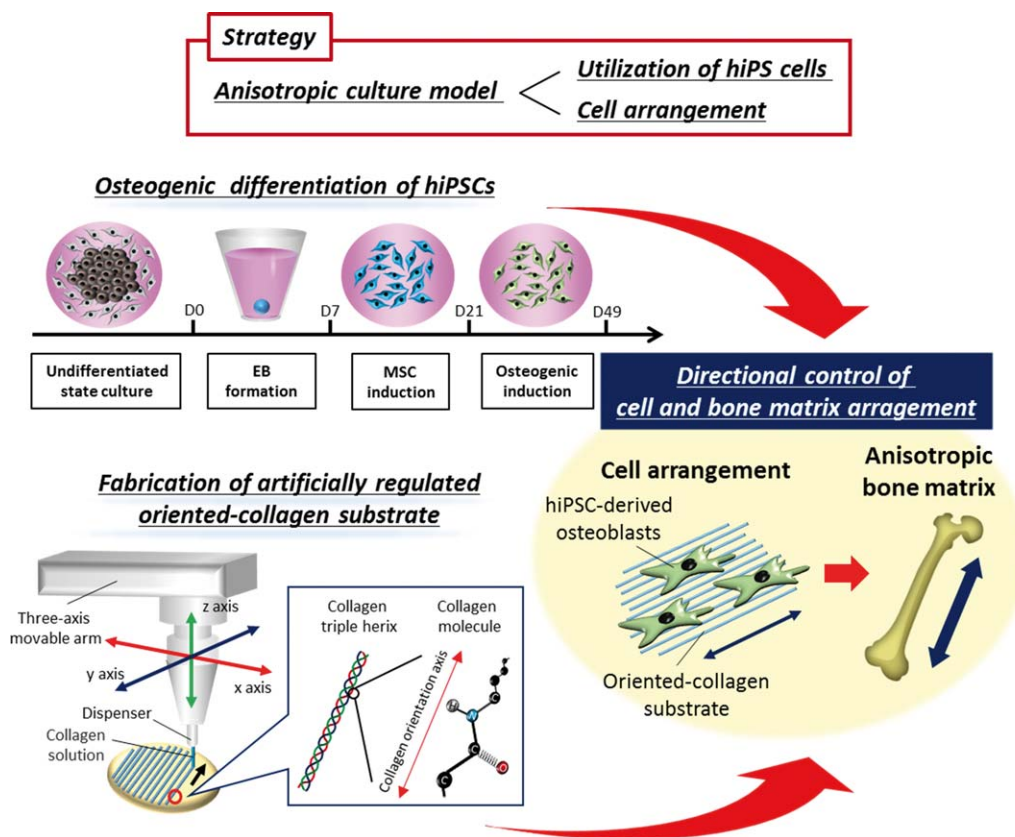


**FIGURE 1.** A schematic diagram, representing the steps for the construction of the anisotropic bone matrix by combining human induced pluripotent stem cells (hiPSCs) and anisotropic culture model, using oriented collagen substrate. Osteogenic differentiation of hiPSCs was induced with three-step culturing method: the expansion of undifferentiated cells, embryoid body (EB) formation for 7 days and mesenchymal stem cell (MSC) induction. Osteogenic induction was performed for 28 days in the osteogenic growth medium. Oriented collagen substrate was artificially fabricated by using a dispense system with three-axis movable arm. Directional control of hiPSC-derived osteoblasts was initiated by oriented collagen substrate.

demonstrated that the aligned osteoblasts can produce the oriented bone matrix<sup>16</sup> depending on the degree of cellular alignment.<sup>17</sup> Therefore, the control of bone tissue anisotropy using iPSCs as a starting material can lead to a breakthrough in bone regenerative medicine, enabling the regeneration of a bone tissue with the proper functions. Oriented collagen substrate, with the architecture quite similar to that of the intact bone matrix, was successfully obtained using a hydrodynamic method.<sup>18,19</sup> Many methods have been developed to generate an anisotropic cell culture platform in tissue engineering, including microfabrication and electrospinning. In this study, we chose a hydrodynamic method to fabricate the oriented collagen substrate. The degree of substrate collagen orientation was shown to be controllable through the modification of the extrusion process of the collagen solution, which allows the development of bone-mimetic structure with different degrees of anisotropy, depending on the anatomical portion.<sup>2</sup> We demonstrated the potential of hiPSC-osteoblasts (OBs) alignment in response to the oriented collagen substrate, using human osteoblasts (hOBs) as controls. Furthermore, the bone matrix architecture induced by hiPSC-OBs was analyzed.

## MATERIALS AND METHODS

### Generation of oriented collagen substrates

Pepsin solubilized porcine skin collagen type I (Nippi, Tokyo, Japan) was prepared at a concentration of 10 mg/mL in 0.02 *N* acetic acid. Oriented collagen substrates were produced using a hydrodynamic extrusion method.<sup>18,19</sup> The deposition of collagen solution into 10× PBS was controlled by a three-axis robotic arm (SM300-3A; Musashi Engineering, Tokyo, Japan), which could regulate the direction of the collagen molecular fiEngin. The deposition speed was set at 400 mm/s. The degree of substrate collagen sheet orientation was controlled more specifically by using a narrower gage needle (22 gage, inner diameter: 0.38 mm) for the extrusion process, as a modification of our previous method.<sup>17</sup> The oriented collagen substrates were prepared by coating the cover glasses (13 mm diameter; Matsunami, Tokyo, Japan) with the obtained collagen sheets.

Molecule orientation of the collagen substrate was analyzed by a birefringence measurement system WPA-micro (Photonic Lattice, Miyagi, Japan) attached to an upright microscope (Olympus, Tokyo, Japan). The specimens were imaged with a 20× objective lens. Data were acquired with three settings of circularly polarized monochromatic light

(laser wave lengths: 523, 543, and 575 nm) for each image. To evaluate the orientation of the birefringence axis, greater index of refraction (the slow axis) was analyzed with WPA-VIEW software (version 2.4.2.9, Photonic Lattice). Since collagen is a positive birefringent material, the polarization axis with slow axis corresponds to the direction of the long axis of collagen fibrils. The three-dimensional imaging and quantification of the surface topographic features were performed by using a three-dimensional (3D) laser microscope (VK-9700; Keyence, Osaka, Japan) and the topographical images of the substrate surfaces were obtained with a scanning pitch of 0.1  $\mu\text{m}$ .

### hiPSCs culture

Human iPS cell line, 201B7, was obtained from Center for iPS Cell Research and Application, Kyoto University, Japan.<sup>9</sup> To maintain the undifferentiated state, hiPSCs were cultured on mitomycin C-treated SNL feeder cells in Primate ES medium (ReproCELL Inc., Yokohama, Japan) supplemented with 4 ng/mL basic fibroblast growth factor (bFGF) (Wako, Osaka, Japan) at 37°C in 5% CO<sub>2</sub>. The medium was replaced daily, and hiPSCs were passaged every 4 days.<sup>20</sup>

### Induction of MSCs differentiation

Induction of MSCs (hiPSC-MSCs) from hiPSCs was performed as described previously<sup>21</sup> with minor modification. Briefly, 5 mM Y-27632 solution (Wako) was added to the undifferentiated hiPSC culture, and the cells were incubated for 1 h prior to the dissociation from culture dish. To form embryoid bodies (EBs), hiPSCs were cultured in suspension for 7 days in low-attachment 96-well plates, in Primate ES medium supplemented with 4 ng/mL bFGF and 5 mM Y-27632. Afterward, 70 EBs were clamped and plated onto 0.1% gelatin-coated culture dishes in MSC growth medium supplemented with  $\alpha$ -MEM (Gibco, Invitrogen, CA), 10% fetal bovine serum (FBS; Gibco), 200 mM L-glutamine (Gibco), 10 mM nonessential amino acid (NEAA; Life technologies, Invitrogen), and cultured for up to 2 weeks at 37°C in 5% CO<sub>2</sub>, until reaching confluence. Culture medium was replaced twice weekly.

### Induction of osteogenic differentiation

Induction of hiPSC-OBs from hiPSC-MSCs was performed as described previously.<sup>22</sup> hiPSC-MSCs were cultured for 4 weeks in osteogenic growth medium supplemented with  $\alpha$ -MEM, 10% FBS, 100 U/mL penicillin, 100  $\mu\text{g}/\text{mL}$  streptomycin, 50  $\mu\text{g}/\text{mL}$  ascorbic acid (Sigma-Aldrich, St. Louis, MO), 10 mM  $\beta$ -glycerol phosphate (Tokyo Kasei, Tokyo, Japan), and 50 nM dexamethasone (MP Bioscience, Solon, OH), at 37°C in 5% CO<sub>2</sub>. Culture medium was refreshed twice weekly.

### hOBs culture

hOBs (Lonza, Basel, Switzerland) were used as a positive control for gene expression analyses and in the cell orientation experiment. According to the provider's instructions, cells were cultured in OGMSingleQuots medium (Lonza)

until confluence, and they were passaged. hOBs were cultured in the same media as used for the iPSC-OBs at 37°C in 5% CO<sub>2</sub>.

### Cell culture on the fabricated anisotropic substrates

The fabricated collagen substrates were sterilized by using short-wavelength ultraviolet (UV-C) germicidal irradiation for 3 min. The hOBs and iPSC-OBs were cultivated at  $2.0 \times 10^4$  cells/mL in  $\alpha$ -MEM supplemented with 10% FBS for 3 days before the morphological analysis. For the analysis of bone matrix under long-term cultivation, the cells were diluted to  $1.0 \times 10^4$  cells/mL and seeded onto the fabricated specimens. The medium was changed twice per week; after culture for 7 days, the medium was supplemented to achieve final concentrations of 50  $\mu\text{g}/\text{mL}$  ascorbic acid (Sigma, St. Louis, MO), 10 mM  $\beta$ -glycerophosphate (Tokyo Kasei, Tokyo, Japan), and 50 nM dexamethasone (MP Bioscience, Solon, OH).

### RNA isolation and quantitative real-time RT-PCR analysis

Total RNA was isolated using Trizol reagent (Invitrogen). Gene expression levels were assessed by using quantitative real-time PCR, in accordance with the manufacturer's instructions (Step-one, Applied Biosystems, Foster City, CA). The threshold cycle (Ct) value was set within the exponential phase of the PCR reaction and the  $\Delta\text{Ct}$  value for each target gene was determined from the subtraction of the Ct value obtained for *GAPDH* (the internal control) from the target gene. The primers and probes for the target genes were supplied by the following Taqman® Gene Expression Assays: *GAPDH*, Hs02758991\_g1; *Col1A1*, Hs00164004\_m1; and *SP7*, Hs01866874\_s1. The results were normalized to the levels of each gene in the control cells.

### Immunocytochemistry

The cultured cells were fixed in 4% formaldehyde/phosphate-buffered saline (PBS) for 20 min. After washing them three times, cells were incubated in PBS/Triton-X (PBST) containing 1% normal goat serum or donkey serum at room temperature for 30 min to block non-specific antibody binding sites. The cells were then incubated with primary antibody at 4°C for 12 h. This was followed by the incubation with a secondary antibody and/or Alexa Fluor 488-conjugated phalloidin (Molecular Probes, Invitrogen). The cells were washed and mounted in ProLong Gold antifade reagent with DAPI (Molecular Probes). Fluorescent images were obtained using a fluorescence microscope (Biozero; Keyence, Osaka, Japan), and processed using Adobe Photoshop 10.0 software (Adobe Systems, San Jose, CA). All immunocytochemical analyses were performed with controlled staining to ensure the antibodies functioned as intended.

### Antibodies

Primary antibodies used in this study were as follows: mouse monoclonal antibody against SSEA-4 (Santa Cruz Biotechnology, Dallas, TX), goat polyclonal antibody against

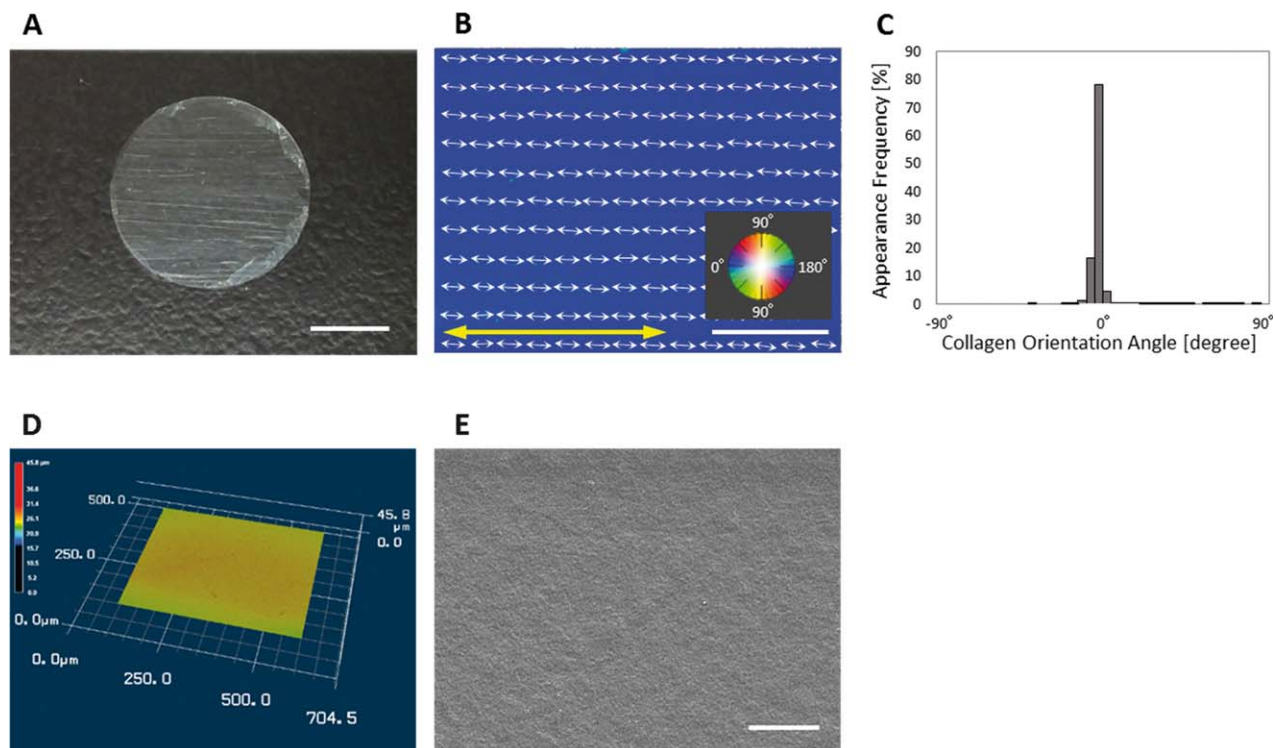


**FIGURE 2.** Fabrication of oriented collagen substrates. (A) Macroscopic image of oriented collagen substrate. Scale bars, 5 mm. (B) Birefringence analysis of oriented collagen substrate. White arrows and color indicate the orientation of collagen fibers. Yellow bidirectional arrow, the direction of the collagen extrusion. Scale bars, 100  $\mu\text{m}$ . (C) The distribution histograms of the collagen orientation angle show preferential alignment to 0°. (D) Laser microscopic image of the surface of the fabricated substrate. (E) SEM image of the fabricated collagen substrate. Scale bar: 10  $\mu\text{m}$ .

CD73 (Santa Cruz Biotechnology), mouse monoclonal antibody against alkaline phosphatase (ALP; Novus, Littleton, CO), rabbit polyclonal antibody against osteopontin (Rockland, PA), and goat polyclonal antibody against collagen type I (Millipore, Ramona, CA). Secondary antibodies used were as follows: Alexa Fluor 488-conjugated goat anti mouse IgG, Alexa Fluor 488-conjugated donkey anti goat IgG, Alexa Fluor 546-conjugated goat anti mouse IgG, and Alexa Fluor 546-conjugated goat anti rabbit IgG (Invitrogen).

#### Quantitative analysis of the degree of cell orientation

Cells cultured on oriented collagen substrates for 3 days were visualized by immunocytochemical analyses. Cells were imaged by using a fluorescence microscope (Biozero, Keyence, Osaka, Japan), processed using ImageJ software (NIH, Rockville, MD). The cell orientation angle ( $\theta$ ) against the axis of substrate collagen arrangement was analyzed using Cell Profiler software (Broad Institute Cambridge, Cambridge, MA). Five replicate measurements were obtained for each group.

To evaluate the degree of cell arrangement, the orientation order parameter  $f_{\theta}$  was calculated.<sup>23</sup> This system was derived by using a distribution function  $n(\theta)$ , which is defined as the number of measured cells at the angle  $\theta$ . The expectation value of the mean square of cosine  $\langle \cos^2\theta \rangle$  and  $f_{\theta}$  can be characterized as follows:

$$\langle \cos^2\theta \rangle = \int_0^{2\pi} \cos^2\theta \cdot n(\theta) / \int_0^{2\pi} n(\theta) d\theta \quad (1)$$

$$f_{\theta} = 2(\langle \cos^2\theta \rangle - 0.5) \quad (2)$$

The degree of cell alignment  $f_{\theta}$  takes a value ranging from  $-1$  (cells perfectly aligned perpendicular to the collagen orientation),  $0$  (cells oriented randomly), to  $1$  (cells perfectly aligned parallel to the collagen orientation).

**Scanning electron microscopy (SEM).** The arrangement of the extracellular matrix secreted by cells was observed by using SEM (JSM-6390; JEOL, Tokyo, Japan). The specimens were rinsed in 0.1 M sodium cacodylate buffer three times, fixed with 2% glutaraldehyde in cacodylate buffer at 4°C for 30 min, and washed with the same buffer. After postfixation with 1% osmium trioxide for 1 h, the specimens were dehydrated with a graded ethanol series (50%–100%) at 5-min intervals, and treated by 100% *t*-butyl alcohol/100% ethanol for 30 min followed by 100% *t*-butyl alcohol. Specimens were freeze-dried, sputter-coated with gold/palladium and analyzed by SEM.

**Statistical analysis.** The analysis of statistical significance was performed using Student's *t* test.  $p < 0.05$  was considered significant.

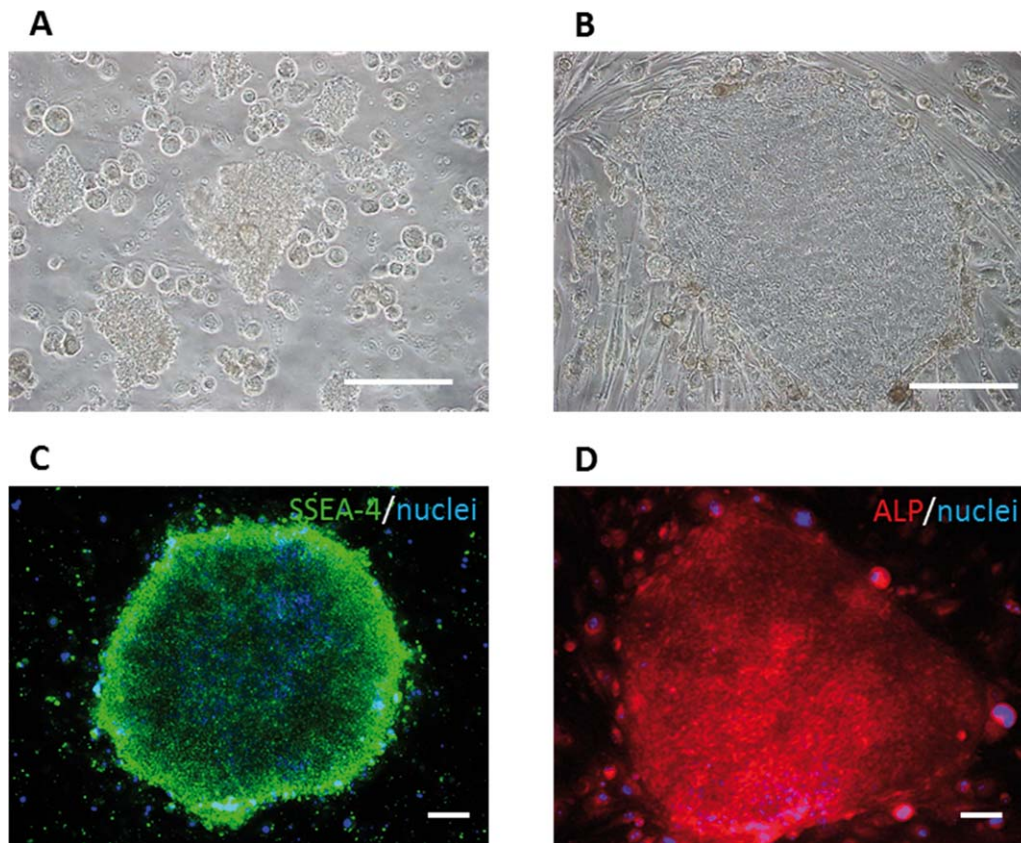


**FIGURE 3.** Undifferentiated human induced pluripotent stem cells (hiPSCs). Phase-contrast images of hiPSC colonies (A) immediately after seeding and (B) after 4 days of culturing on SNL feeder cells. Immunocytochemical images of hiPSC colonies stained for (C) SSEA-4 (green) and (D) alkaline phosphatase (red). Blue, nuclei. Scale bars, 100  $\mu\text{m}$ .

## RESULTS

### Fabrication of oriented collagen substrates

The macroscopic image of the fabricated collagen substrate is shown in Figure 2A. Orientation map image and the distribution histogram of substrate collagen orientation are presented in Figure 2B, C. The angular distribution of collagen molecules demonstrated that the collagen fibers in the fabricated collagen substrate have a strongly-oriented arrangement. Laser microscope analysis revealed that the fabricated substrates have a relatively smooth surface structure without significant roughness ( $R_a = 0.43 \mu\text{m}$ ) (Fig. 2D). The SEM image of the fabricated oriented collagen substrate is shown in Figure 2E. The each collagen fiber exhibited tightly connected networks.

### hiPSCs culture in an undifferentiated state

hiPSCs attached to feeder cells immediately after thawing (Fig. 3A), and cell colonies developed after 4 days (Fig. 3B). The obtained hiPSCs colonies were positive for SSEA-4 and ALP, positive markers for undifferentiated stem cells (Fig. 3C, D).

### Induction of hiPSC-MSCs

EBs, observed in the floating culture of Y27632-treated hiPSCs, were shown to be large (approximately 500  $\mu\text{m}$  in diameter), with a uniform morphology (Fig. 4A). After

plating the EBs on the gelatin-coated culture dish, cells migrated from EBs under the MSC growth condition (Fig. 4B), and reached confluence after 2 weeks of culturing (Fig. 4C). These cells exhibited fibroblastic-like morphology and they were shown to express CD73, a surface antigen specific to MSCs (Fig. 4D).

### Induction of hiPSC-OBs

As shown in Figure 5A, osteogenic-induced hiPSCs were positive for the expression of collagen type I and osteopontin, osteogenic markers, whereas hiPSC-MSCs did not express these molecules. Furthermore, osteogenic-induced hiPSCs were positive for ALP activity, an osteogenic marker; whereas hiPSC-MSCs were negative (Fig. 5B). Gene expression analysis revealed that *SP7* (osterix) and *COL1a1* (collagen type I) were expressed in osteogenic-induced hiPSCs at the same level as in the hOBs (Fig. 6A).

### Control of hiPSC-OBs arrangement and construction of oriented bone matrix

hiPSC-OBs and hOBs both showed preferential alignment along collagen orientation. The degree of cell alignment  $f_\theta$  was shown not to differ significantly between hiPSC-OBs ( $f_\theta = 0.65 \pm 0.11$ ) and hOBs ( $f_\theta = 0.49 \pm 0.13$ ) (Fig. 6B). In addition, the other cell adhesion parameters, including cell spreading area and aspect ratio, were not significantly

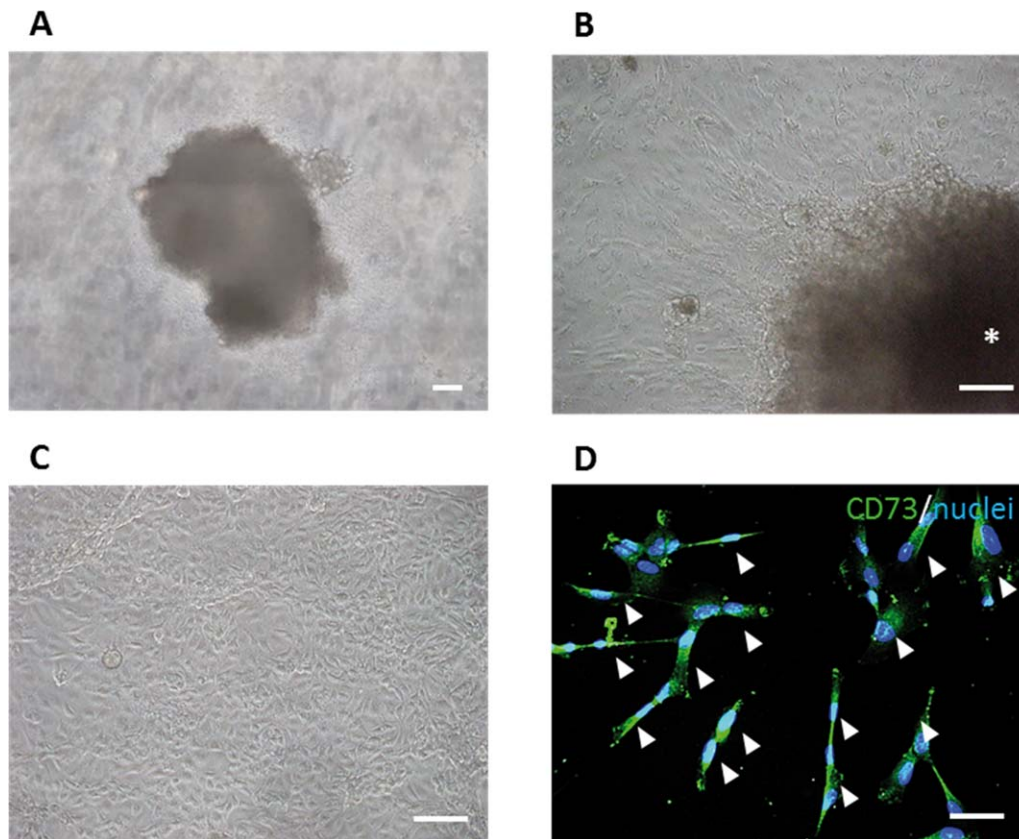


**FIGURE 4.** Differentiation of human mesenchymal stem cells (hMSCs) from human induced pluripotent cells (hiPSCs). (A) Embryoid bodies (EBs) formed in the suspension culture. (B) Cells migrated from EBs cultured using MSC growth medium and (C) reached confluence after 2 weeks. \*, EBs. (D) Immunocytochemical images obtained after the staining of EBs with CD73 (green). Blue, nuclei. Scale bars, 100  $\mu\text{m}$ .

different between hiPSC-OBs and hOBs (Fig. 6C). The SEM observations of the long-term culture revealed that the extracellular collagen fiber matrix secreted by hiPSC-OBs was aligned along the direction of hiPSC-OBs arrangement (Fig. 6D). The secreted collagen fibers could be clearly distinguished from the bare scaffold without cells because of the difference in their fibrous formation.

## DISCUSSION

For the clinical use of hiPSCs, homogeneous differentiation of hiPSCs into hiPSC-OBs is important to prevent the development of teratogenic cells. Here, osteogenic differentiation of hiPSCs was performed in accordance with previously established methodology,<sup>21,22</sup> with some modifications, by using a three-step culture processes: culture of hiPSCs in an undifferentiated state, the induction of MSC differentiation through EB formation, and the induction of osteogenic differentiation. We optimized the osteogenic differentiation process from hiPSCs by the combination of pre-treatment of hiPSCs with ROCK inhibitor Y-27632 and EBs formation. Pluripotency of hiPSCs was maintained by using SNL fibroblasts as feeder cells (Fig. 3A, B). Because the excess period of culture induces deviation from the undifferentiated state, especially in the central region of hiPSC colonies on SNL feeder cells, hiPSCs were passaged every 4 days, which allowed the expanding of hiPSCs in an undifferentiated state

(Fig. 3C, D). MSC differentiation was induced through the formation of EBs in the floating culture. The pre-treatment of hiPSCs with Y-27632 inhibited cell apoptosis and promoted the agglomeration of dissociated hiPSCs,<sup>24</sup> which lead to the formation of EBs of uniform size and morphology (Fig. 4A), which is crucial for efficient differentiation. Cells migrating from the EBs exhibited fibroblastic-like morphology (Fig. 4C, D), resembling human primary MSCs.<sup>25</sup> Moreover, the expression of CD73, a marker specific for MSCs was observed, indicating the successful induction of hiPSC-MSCs. Osteoblast differentiation was subsequently induced by using osteogenic differentiation condition. During osteoblastic differentiation, genes encoding bone extracellular matrix proteins are activated sequentially at each phase of differentiation,<sup>26</sup> including proliferation, matrix development, and mineralization phases. Collagen type I and osteopontin, the markers of the early stage of osteogenic differentiation, were shown to be expressed in hiPSC-MSCs cultured in osteogenic growth medium (Fig. 5A). The assessment of ALP activity, which is an indicator of the progression of osteogenic differentiation, also demonstrated the osteoblastic potential of hiPSC-OBs (Fig. 5B). Because ALP functions as a positive marker for both stem cells and osteogenic cells, the osteogenic gene expression properties of the obtained hiPSC-OBs were compared with those of the hOBs, in addition to the assessment of ALP expression. The

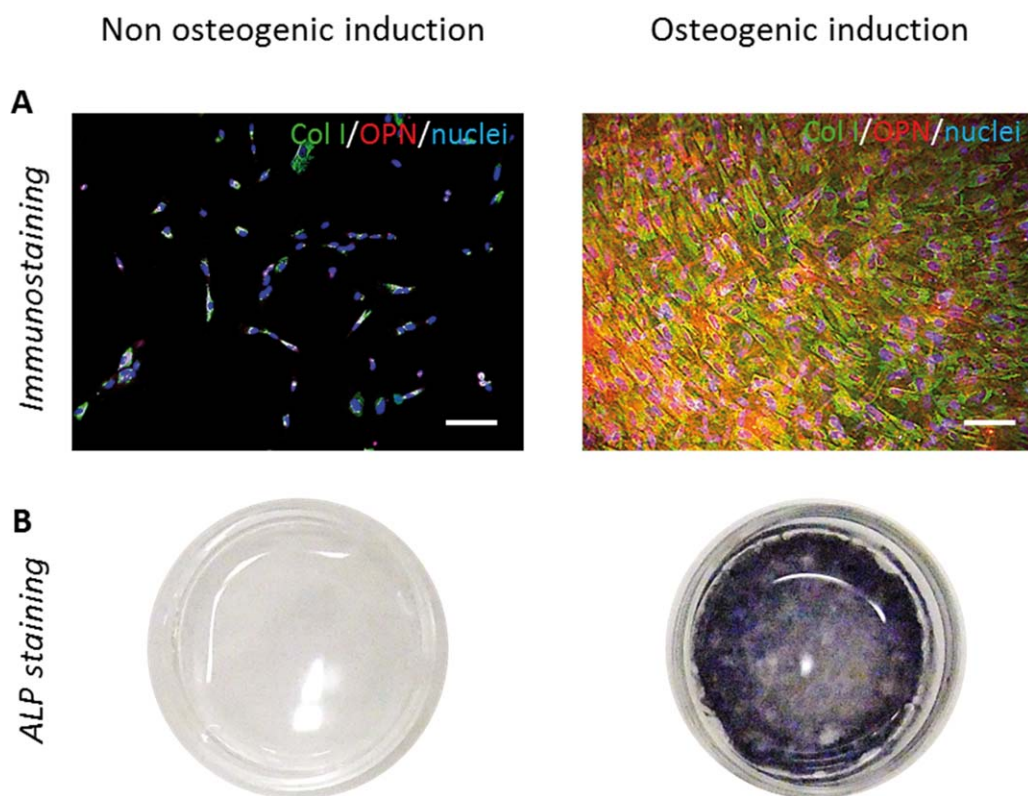


**FIGURE 5.** Osteogenic differentiation from human induced mesenchymal stem cells (hiPSC-MSCs). (A) Immunocytochemical analysis of hiPSC-MSCs maintained in MSC growth conditions (left, non-osteogenic induction) and under osteogenic growth conditions (right, osteogenic induction). Green, collagen type I; red, osteopontin; blue, DAPI. Scale bars, 100  $\mu\text{m}$ . (B) ALP staining of hiPS-MSCs cultured for 2 weeks in MSC growth medium (left, non-osteogenic induction) and under osteogenic growth conditions (right, osteogenic induction).

expression levels of osterix and collagen type I were shown to be similar to the levels of these molecules detected in hOBs (Fig. 6A), which indicated the successful development of osteoblasts from hiPSC-MSCs. Taken together, these results demonstrate that the osteogenic differentiation from hiPSCs was successfully controlled.

The control of both differentiation and morphological arrangement are an absolute imperative for appropriate bone tissue regeneration. Biomaterial design for the regeneration of anisotropic bone microstructure should be established in the field of bone regenerative medicine. Since the microarchitecture of bone matrix is determined by the osteoblast arrangement, the control of this process in a desired direction and degree from hiPSCs have a great potential in supporting the next stage of tissue engineering. Most interestingly, we have demonstrated that the degree of bone apatite orientation to be controllable by regulating the level of osteoblast arrangement.<sup>17</sup>

Collagen has been used in biomedicine due to its favorable structural and biological characteristics, which allow the maintenance of cellular intrinsic functions.<sup>27–29</sup> In this study, we established a powerful strategy through the combination of the oriented collagen substrate and hiPSC cultivation (Fig. 1). The obtained collagen substrates showed strong retardation, which indicated that the fabricated scaffolds have a highly anisotropic molecular arrangement derived from the collagen fiber alignment (Fig. 2B). The

distribution analysis of collagen molecular orientation revealed that the collagen molecules show uniform orientation depending on the direction of collagen solution extrusion (Fig. 2C).

We successfully controlled the arrangement of iPSC-OBs along the substrate collagen orientation. Notably, hiPSC-OBs showed preferential alignment comparable to that of hOBs with actin stress fibers elongating along the direction of cell arrangement (Fig. 6B). These results indicate that the obtained hiPSC-derived osteoblasts demonstrate a potential to respond to the external anisotropic microenvironment and generate the cellular assembly similar to that of the somatic cells. The successful control of iPSC-OBs arrangement is considered to be derived from the interaction between substrate collagen molecule and cell surface via integrin receptors.<sup>30</sup> Integrins are transmembrane receptors and their signaling is related with cytoskeletal organization, gene expression, and diverse cellular functions, in which they are involved by transmitting extracellular information into intracellular actin fibers.<sup>31</sup> hiPSC-OBs can sense the anisotropic orientation of collagen molecules through integrins, which leads to the reorganization of their morphologies and results in the preferential cell arrangement along the direction of the substrate collagen, but not completely parallel to the substrate collagen fibers. Moreover, hiPSC-OBs demonstrated normal adhesion behaviors, as evidenced by the analysis of adhesion area and cell aspect ratio (Fig. 6C).

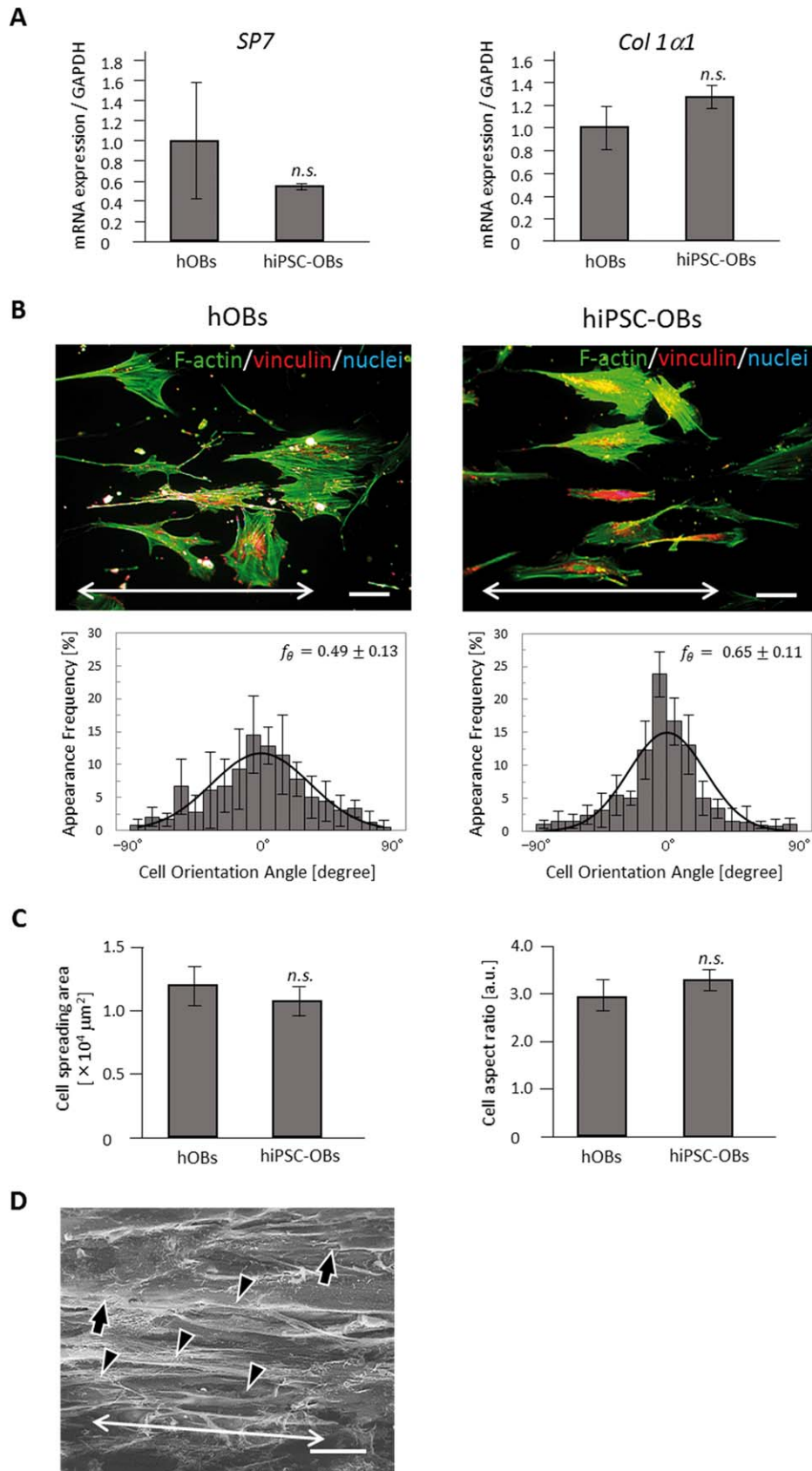


**FIGURE 6.** Construction of human induced pluripotent stem cell-derived anisotropic bone matrix. (A) The analysis of osteogenic marker genes, SP7 (left) and COL1a1 (right), in human osteoblasts (hOBs) and human induced mesenchymal stem cells (hiPSC-MSCs) following the osteogenic induction. Expression levels (mean  $\pm$  standard deviation, SD) of these genes were normalized to GAPDH levels. Error bars, SD; n.s., no statistically significant difference observed. (B) Immunocytochemical analyses and the distribution histograms of cell orientation obtained for hOBs (left) and human induced pluripotent stem cell-derived osteoblasts (hiPSC-OBs; right). Bidirectional arrows in (B) indicate the axis of substrate collagen orientation. Green, F-actin; red, vinculin; blue, nuclei. Scale bars, 100  $\mu\text{m}$ . (C) The comparison of cell spreading area (left) and cell aspect ratio (right) between hOBs and hiPSC-OBs. (D) Scanning electron microscope image (magnification, 5000 $\times$ ) of hiPSC-OBs and secreted collagen fibers on the oriented collagen substrates. Arrows, osteoblasts cultured on the substrate. Arrowheads, secreted collagen matrix. Bidirectional arrow, the orientation of collagen fibers secreted by hiPSC-OBs. Scale bars, 50  $\mu\text{m}$ .



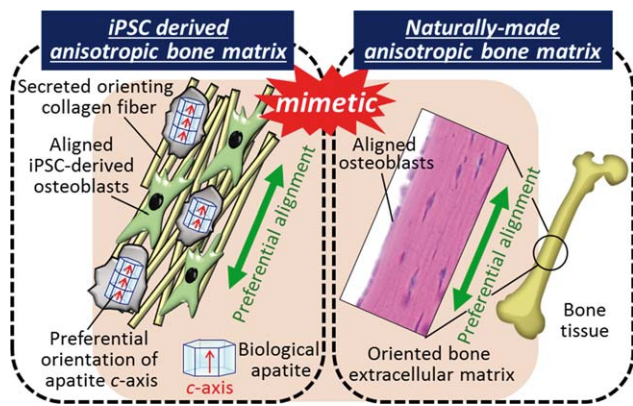


**FIGURE 7.** A schematic illustration showing the establishment of the anisotropic bone matrix microstructure from the induced pluripotent stem cells (iPSCs). The bone-mimetic anisotropic bone matrix architecture was successfully generated by controlling the human induced pluripotent stem cell-derived osteoblast (hiPSC-OB) arrangement.

Recently, due to the ability to promote osteogenic differentiation, polymeric matrix produced by electrospinning have been used often as scaffold for the iPS culturing. Polycaprolactone (PCL) scaffolds<sup>32</sup> and polyethersulfone (PES) of nanofiber-based scaffolds<sup>33</sup> were shown to promote the osteogenic differentiation of iPSCs. D'Angelo et al. demonstrated that nanofiber-based scaffolds of poly-L-lactic acid (PLLA) combined with hydroxyapatite successfully induce osteogenic differentiation of murine iPSCs and ESCs without exogenous factors for osteogenesis.<sup>34</sup> They speculated that a direct interaction between the seeded stem cells and PLLA/HAp substrates is a key factor promoting osteogenic differentiation. However, even these advanced bone regenerative techniques cannot promote the anisotropic regeneration of bone tissue, which is crucial for the retrieval of the original bone function.<sup>2,3</sup> Additionally, during the early stages of the natural regeneration process, the collagen matrix secreted by osteoblasts shows random, disorganized microstructure, which impairs mechanical function because of the disrupted mechanosensing by osteocytes owing to the insufficient recovery of bone mass.<sup>35</sup> The present strategy, which used hiPSCs and artificially oriented collagen substrate, enabled the successful control of the bone matrix alignment process, leading to healthy bone recovery with appropriate anisotropy. The present work will allow autografts from patient-specific induced pluripotent stem (iPS) cells for bone therapy.

Here, by focusing on the specific interaction between the integrins and the amino acid sequence of collagen fibers,<sup>36,37</sup> the orientation of iPSC-OBs was artificially regulated. Interestingly, the collagen matrix secreted by hiPSC-OBs was synchronously aligned with the cellular orientation (Fig. 6D), suggesting that the anisotropic bone matrix was successfully constructed by regulating the arrangement of hiPSC-OBs (Fig. 7). Mineralization proceeded along the collagen fiber matrix as a template and the apatite crystallize along the secreted collagen fibers. Indeed, our previous research revealed the correlation between cell alignment and the crystallographic orientation of apatite.<sup>17</sup> Further

cultivation could realize the oriented apatite crystal formation from hiPSC and the findings will be published in subsequent reports.

The fabricated collagen substrates showed a relatively smooth surface with negligible roughness, which indicated that the molecular orientation of the collagen had significant effects on the control of the cell ordering fate. On the other hand, the surface topography also plays important roles in the determination of the cell orientation and tissue construction. We previously achieved the control of the bone matrix anisotropy by using surface patterning,<sup>38,39</sup> which indicated that the interface structure between the materials and cells could also play a key role in the construction of oriented tissue microstructure.

Although iPSCs are a promising tool for tissue regeneration, the insufficient functionality of iPSC-derived cells remains an issue.<sup>40</sup> In this study, the iPSC-OBs were shown to possess a prominent level of intact functionality, allowing them to regulate cell alignment, which leads to the construction of bone-mimetic anisotropic microstructure. These results indicate that the osteoblasts differentiated from the reprogrammed cells using Oct3/4, Sox2, Klf4, and c-Myc, can potentially control their arrangement in response to the spatial orientation of amino acid sequence in collagen molecule.

Considering that the majority of biological tissues or organs have anisotropic microstructure, including blood vessel,<sup>41</sup> tendon,<sup>42</sup> and skeletal muscle,<sup>43</sup> our approach can represent a powerful strategy for the construction of various types of organs, maintaining their original functionality following the process of regeneration. The anisotropic culture system with tissue-specific differentiation methodology established in this study represent a crucial breakthrough and a new strategy for tissue-specific regeneration.

## CONCLUSION

iPS cells have helped overcome the ethical and immunogenic problems associated with the ES cells and currently, several types of tissues or organs can be obtained from the somatic cells of patients by controlling the differentiation processes. A strategy essential for the improvement of the regenerative medicine approaches is the development of the organ-specific microstructure that allows the expression of the original function of these tissues. In this study, the anisotropic microstructure of bone matrix that governs the mechanical function of bone was established by controlling hiPSCs-derived osteoblasts. The obtained hiPSC-OBs were shown to be aligned preferentially along the substrate collagen orientation, which was followed by the construction of anisotropic collagen matrix along cellular orientation. To the best of our knowledge, this is the first report to achieve the generation of anisotropic bone collagenous matrix microstructure from hiPSCs, providing a novel strategy for the regeneration of tissues with their appropriate architecture and functionality.

## ACKNOWLEDGMENTS

This work was supported by the Grants-in-Aid for Scientific Research (S) from the Japan Society for Promotion of Science.

## REFERENCES

- Weiner S, Wagner HD. The material bone: Structure mechanical function relations. *Annu Rev Mater Sci* 1998;28:271–298.
- Nakano T, Kaibara K, Tabata Y, Nagata N, Enomoto S, Marukawa E, Umakoshi Y. Unique alignment and texture of biological apatite crystallites in typical calcified tissues analyzed by microbeam X-ray diffractometer system. *Bone* 2002;31:479–487.
- Ishimoto T, Nakano T, Umakoshi Y, Yamamoto M, Tabata Y. Degree of biological apatite c-axis orientation rather than bone mineral density controls mechanical function in bone regenerated using recombinant bone morphogenetic protein-2. *J Bone Miner Res* 2013;28:1170–1179.
- Shiraishi A, Miyabe S, Nakano T, Umakoshi Y, Ito M, Mihara M. The combination therapy with alfacalcidol and risedronate improves the mechanical property in lumbar spine by affecting the material properties in an ovariectomized rat model of osteoporosis. *BMC Musculoskelet Disord* 2009;10:13.
- Lee JW, Nakano T, Toyosawa S, Tabata Y, Umakoshi Y. Areal distribution of preferential alignment of biological apatite (BAP) crystallite on cross-section of center of femoral diaphysis in osteopetrotic (op/op) mouse. *Mater Trans* 2007;48:337–342.
- Nakano T, Kaibara K, Ishimoto T, Tabata Y, Umakoshi Y. Biological apatite (BAP) crystallographic orientation and texture as a new index for assessing the microstructure and function of bone regenerated by tissue engineering. *Bone* 2012;51:741–747.
- Sekita A, Matsugaki A, Ishimoto T, Nakano T. Synchronous disruption of anisotropic arrangement of the osteocyte network and collagen/apatite in melanoma bone metastasis. *J Struct Biol* 2017;197:260–270.
- Takahashi K, Yamanaka S. Induction of pluripotent stem cells from mouse embryonic and adult fibroblast cultures by defined factors. *Cell* 2006;126:663–676.
- Takahashi K, Tanabe K, Ohnuki M, Narita M, Ichisaka T, Tomoda K, Yamanaka S. Induction of pluripotent stem cells from adult human fibroblasts by defined factors. *Cell* 2007;131:861–872.
- Park S, Im G. Embryonic stem cells and induced pluripotent stem cells for skeletal regeneration. *Tissue Eng* 2014;20:381–391.
- Bock C, Kiskinis E, Verstappen G, Gu HC, Boulting G, Smith ZD, Ziller M, Croft GF, Amoroso MW, Oakley DH, Gnirke A, Eggan K, Meissner A. Reference maps of human ES and iPS cell variation enable high-throughput characterization of pluripotent cell lines. *Cell* 2011;144:439–452.
- Wu Q, Yang B, Hu k, Cao C, Man Y, Wang P. Deriving osteogenic cells from induced pluripotent stem cells for bone tissue engineering. *Tissue Eng* 2017;23:1–8.
- Lou XX. Induced pluripotent stem cells as a new strategy for osteogenesis and bone regeneration. *Stem Cell Rev Rep* 2015;11:645–651.
- Chamberlain G, Fox J, Ashton B, Middleton J. Concise review: Mesenchymal stem cells: Their phenotype, differentiation capacity, immunological features, and potential for homing. *Stem Cells* 2007;25:2739–2749.
- Murphy SV, Atala A. Organ engineering - combining stem cells, biomaterials, and bioreactors to produce bioengineered organs for transplantation. *BioEssays* 2013;35:163–172.
- Matsugaki A, Fujiwara N, Nakano T. Continuous cyclic stretch induces osteoblast alignment and formation of anisotropic collagen fiber matrix. *Acta Biomater* 2013;9:7227–7235.
- Matsugaki A, Isobe Y, Saku T, Nakano T. Quantitative regulation of bone-mimetic, oriented collagen/apatite matrix structure depends on the degree of osteoblast alignment on oriented collagen substrates. *J Biomed Mater Res Part A* 2015;103:489–499.
- Kirkwood JE, Fuller GG. Liquid crystalline collagen: A self-assembled morphology for the orientation of mammalian cells. *Langmuir* 2009;25:3200–3206.
- Isobe Y, Kosaka T, Kuwahara G, Mikami H, Saku T, Kodama S. Oriented collagen scaffolds for tissue engineering. *Materials* 2012;5:501–511.
- Takahashi K, Okita K, Nakagawa M, Yamanaka S. Induction of pluripotent stem cells from fibroblast cultures. *Nat Protoc* 2007;2:3081–3089.
- Villa-Diaz LG, Brown SE, Liu Y, Ross AM, Lahann J, Parent JM, Krebsbach PH. Derivation of mesenchymal stem cells from human induced pluripotent stem cells cultured on synthetic substrates. *Stem Cells* 2012;30:1174–1181.
- Brown SE, Tong W, Krebsbach PH. The derivation of mesenchymal stem cells from human embryonic stem cells. *Cells Tissues Organs* 2009;189:256–260.
- Umeno A, Kotani H, Iwasaka M, Ueno S. Quantification of adherent cell orientation and morphology under strong magnetic fields. *IEEE Trans Magn* 2001;37:2909–2911.
- Horiguchi A, Yazaki K, Aoyagi M, Ohnuki Y, Kurosawa H. Effective Rho-associated protein kinase inhibitor treatment to dissociate human iPS cells for suspension culture to form embryoid body-like cell aggregates. *J Biosci Bioeng* 2014;118:588–592.
- Romanov YA, Svintsitskaya VA, Smirnov VN. Searching for alternative sources of postnatal human mesenchymal stem cells: Candidate MSC-like cells from umbilical cord. *Stem Cells* 2003;21:105–110.
- Aubin JE. Regulation of osteoblast formation and function. *Rev Endocr Metab Disord* 2001;2:81–94.
- Chattopadhyay S, Raines RT. Collagen-based biomaterials for wound healing. *Biopolymers* 2014;101:821–833.
- Lee KW, Lee JS, Jang JW, Shim YB, Lee K-I. Tendon-bone interface healing using an injectable rhBMP-2-containing collagen gel in a rabbit extra-articular bone tunnel model. *J Tissue Eng Regen Med* 2015;11:1435–1441.
- Yang XB, Bhatnagar RS, Li S, Oreffo ROC. Biomimetic collagen scaffolds for human bone cell growth and differentiation. *Tissue Eng* 2004;10:1148–1159.
- Docheva D, Popov C, Alberton P, Aszodi A. Integrin signaling in skeletal development and function. *Birth Defects Res C Embryo Today* 2014;102:13–36.
- Boudreau J, Jones PL. Extracellular matrix and integrin signalling: The shape of things to come. *Biochem J* 1999;339:481–488.
- Jin GZ, Kim TH, Kim JH, Won JE, Yoo SY, Choi SJ, Hyun JK, Kim HW. Bone tissue engineering of induced pluripotent stem cells cultured with macrochanneled polymer scaffold. *J Biomed Mater Res A* 2013;101:1283–1291.
- Ardehshirylajimi A, Hosseinkhani S, Parivar K, Yaghmaie P, Soleimani M. Nanofiber-based polyethersulfone scaffold and efficient differentiation of human induced pluripotent stem cells into osteoblastic lineage. *Mol Biol Rep* 2013;40:4287–4294.
- D'Angelo F, Armentano I, Cacciotti I, Tiribuzi R, Quattrocchi M, Del Gaudio C, Fortunati E, Saino E, Caraffa A, Cerulli GG, Visai L, Kenny JM, Sampaolesi M, Bianco A, Martino S, Orlicchio A. Tuning multi/pluri-potent stem cell fate by electrospun poly(L-lactic acid)-calcium-deficient hydroxyapatite nanocomposite Mats. *Biomacromolecules* 2012;13:1350–1360.
- Ishimoto T, Nakano T, Umakoshi Y, Yamamoto M, Tabata Y. Role of stress distribution on healing process of preferential alignment of biological apatite in long bones. *Mat Sci Forum* 2006;512:261–264.
- Taubenberger AV, Woodruff MA, Bai HF, Muller DJ, Hutmacher DW. The effect of unlocking RGD-motifs in collagen I on pre-osteoblast adhesion and differentiation. *Biomaterials* 2010;31:2827–2835.
- Yamazaki CM, Kadoya Y, Hozumi K, Okano-Kosugi H, Asada S, Kitagawa K, Nomizu M, Koide T. A collagen-mimetic triple helical supramolecule that evokes integrin-dependent cell responses. *Biomaterials* 2010;31:1925–1934.
- Matsugaki A, Aramoto G, Ninomiya T, Sawada H, Hata S, Nakano T. Abnormal arrangement of a collagen/apatite extracellular matrix orthogonal to osteoblast alignment is constructed by a nanoscale periodic surface structure. *Biomaterials* 2015; 37:134–143.
- Matsugaki A, Aramoto G, Nakano T. The alignment of MC3T3-E1 osteoblasts on steps of slip traces introduced by dislocation motion. *Biomaterials* 2012;33:7327–7335.
- Savla JJ, Nelson BC, Perry CN, Adler ED. Induced pluripotent stem cells for the study of cardiovascular disease. *J Am Coll Cardiol* 2014;64:512–519.
- Gasser TC, Ogden RW, Holzapfel GA. Hyperelastic modelling of arterial layers with distributed collagen fibre orientations. *J R Soc Interface* 2006;3:15–35.
- Kannus P. Structure of the tendon connective tissue. *Scand J Med Sci Sports* 2000;10:312–320.
- Lieber RL, Friden J. Functional and clinical significance of skeletal muscle architecture. *Muscle Nerve* 2000;23:1647–1666.